

Research Article

Nonclassical Parametric Variational Technique to Manipulability Control of a Serial-Link Robot That Is Used in Treatment of Femoral Shaft Fractures

Ghazwa F. Abd 

Department of Mathematics, College of Science, Mustansiriyah University, Baghdad, Iraq

Correspondence should be addressed to Ghazwa F. Abd; k.abd@uomustansiriyah.edu.iq

Received 31 January 2023; Revised 12 July 2023; Accepted 29 July 2023; Published 28 October 2023

Academic Editor: Waleed Adel

Copyright © 2023 Ghazwa F. Abd. This is an open access article distributed under the Creative Commons Attribution License, which permits unrestricted use, distribution, and reproduction in any medium, provided the original work is properly cited.

Robot-assisted intramedullary nailing is a minimally invasive surgical procedure commonly used to treat femur fractures. Despite its benefits, there are several disadvantages associated with this technique, such as frequent malalignment, physical fatigue, and excessive radiation exposure for medical personnel. Therefore, it is crucial to ensure that robotic surgery for fracture reduction is precise and safe. Precise calculation and regulation of the robot's reduction force are of utmost importance. In this study, we propose a manipulator that utilises robot assistance and indirect contact with the femur to effectively reduce fractures in the shaft. The dynamics of the reduction robot are analysed using the implicit function theorem, which allows us to address the reduced problem. A parametric approach is presented to tackle the initial algebraic constraints, enabling the approximation of the state-space solution while simultaneously controlling the class of constraints in a multiway manner. This approach simplifies the problem from an infinite-dimensional one to a finite-dimensional one, leading to an approximate solution obtained by solving a set of control linear algebraic equations. The proposed robotic-assisted system enhances fracture repositioning while reducing radiation exposure for both the patient and the medical staff. Through numerical results and their practical application, we have developed an efficient method that yields positive outcomes.

1. Introduction

In recent years, there has been a growing trend of analysing and synthesising linear time-invariant control systems in the form of differential-algebraic equations [1–4]. One significant class of these systems, known as DAC-SYS (differential-algebraic control systems), comprises systems controlled by mechanical differential algebra [5–7]. These systems find wide application in various fields, including robot dynamics, machine dynamics, and vehicle dynamics [8–10], with the principles of multibody system theory being employed in each case. When subsystems are coupled by constraints or when kinematic linkages such as joints are utilised, constraint equations can be explicitly incorporated, resulting in a mathematical model with differential-algebraic equations [11, 12]. The physical relevance of DAC-SYS is clearly manifested in this natural system description. The concept of DAC-SYS has been introduced [13–15], and in recent years, tools for simulation, identification,

analysis, and design of these systems have been developed. The algorithms for numerical simulation are addressed [16, 17], while for mechanical DAC-SYS, a recent study focuses on the design and manipulability analysis of a serial-link robot (S-LR) [18–20]. This paper is aimed at investigating the kinematics of the robotic DAC-SYS, specifically under the influence of algebraic kinematic constraints at the joints. This information allows critical points of the variational formulation to be determined, and all efficiency functions with consistent initial conditions can be consolidated into a performance index. This motivated our research to identify the optimal control method for a robotic manipulation system subject to S-LR constraints.

2. Manipulability Analysis and Inverse Kinematics

Finding a workspace representation appropriate for regulating end effector motion is the main goal of this section.

Dexterity and maneuverability must be quantified in order to plan tasks that include positioning and orienting the robot's end tip as well as for the design and control of the robot. It is additionally helpful for planning trajectories and computing inverse kinematics. For assessing a robot's capacity to move around a workplace, manipulability measurement is very crucial.

Figure 1 illustrates the manipulator's coordinate systems.

The robot's velocity can be determined by Jacobian from the joint velocities using the following notation for the manipulator tip's kinematic equation expressed by $V = F(W)$, where $V \in \mathbb{R}^6$ is the robot tip's operational spatial vector, $W \in \mathbb{R}^6$ is the joint's spatial vector, and F stands for transfer function.

The robot's differential kinematic equation can be expressed as follows:

$$V = J(W)W, \quad (1)$$

with

$$J(W) = \begin{bmatrix} \frac{\partial F_1}{\partial W_1} & \frac{\partial F_1}{\partial W_2} & \dots & \frac{\partial F_1}{\partial W_6} \\ \frac{\partial F_2}{\partial W_1} & \frac{\partial F_2}{\partial W_2} & \dots & \frac{\partial F_2}{\partial W_6} \\ \vdots & \vdots & \ddots & \vdots \\ \frac{\partial F_6}{\partial W_1} & \frac{\partial F_6}{\partial W_2} & \dots & \frac{\partial F_6}{\partial W_6} \end{bmatrix}. \quad (2)$$

The vector product method yields the robot's Jacobian matrix as follows:

$$J = \begin{bmatrix} z_0 & z_1 & z_2 & z_3 \times s_6^{0,3} & z_4 \times s_6^{0,4} & z_5 \times s_6^{0,5} \\ 0 & 0 & 0 & z_3 & z_4 & z_5 \end{bmatrix}, \quad (3)$$

where z_i is a joint axis-corresponding unit vector; the vector from the $\{i\}$ -origin coordinate's to the $\{6\}$ -coordinate's origin is represented by $s_6^{0,i}$.

It is possible to formulate equation (3) as

$$J = \begin{bmatrix} 0 & 0 & 1 & 4 & J_1^5 & J_3^4 \\ 0 & -1 & 0 & 0 & -\ell_2 \cos(\vartheta_5) - a_3 \cos(\vartheta_5) & \ell_2 \sin(\vartheta_5) \sin(\vartheta_6) \\ 1 & 0 & 0 & J_3^4 & J_3^5 & J_3^4 \\ 0 & 0 & 0 & 0 & -\cos(\vartheta_4) & \sin(\vartheta_4) \sin(\vartheta_5) \\ 0 & 0 & 0 & -1 & 0 & \cos(\vartheta_5) \\ 0 & 0 & 0 & 0 & -\sin(\vartheta_4) & -\cos(\vartheta_4) \sin(\vartheta_5) \end{bmatrix}, \quad (4)$$

where

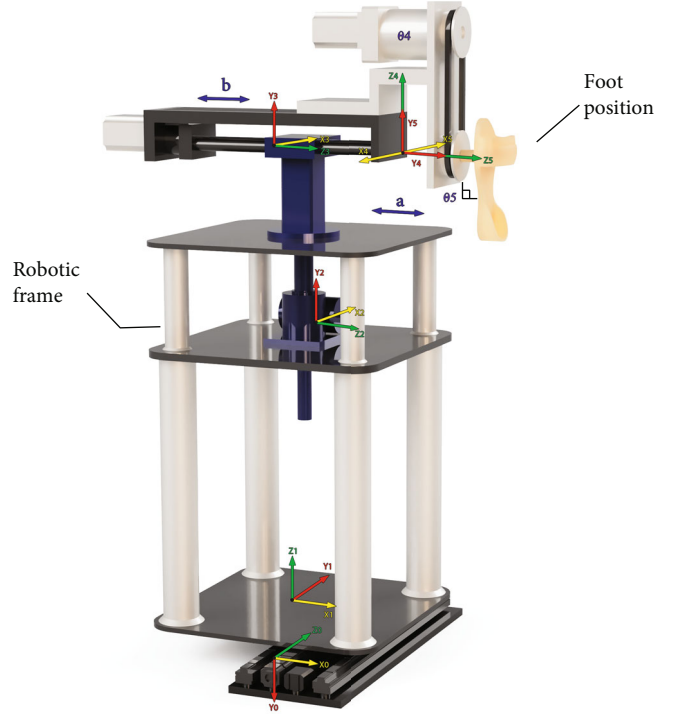


FIGURE 1: Link coordinate system of the robotic manipulator.

$$\begin{cases} J_1^4 = \ell_2 \cos(\vartheta_4) \cos(\vartheta_5) \cos(\vartheta_6) + a_3 \cos(\vartheta_4) \cos(\vartheta_5) + \ell_2 \sin(\vartheta_4) \sin(\vartheta_6) + \ell_2 \sin(\vartheta_4), \\ J_1^5 = -\ell_2 \sin(\vartheta_4) \sin(\vartheta_5) \sin(\vartheta_6) - a_3 \sin(\vartheta_4) \sin(\vartheta_5), \\ J_1^6 = -\ell_2 \cos(\vartheta_4) \cos(\vartheta_6) - \ell_2 \sin(\vartheta_4) \cos(\vartheta_5) \sin(\vartheta_6), \\ J_3^4 = \ell_2 \sin(\vartheta_4) \cos(\vartheta_5) \cos(\vartheta_6) + a_3 \sin(\vartheta_4) \cos(\vartheta_5) - \ell_2 \cos(\vartheta_4) \sin(\vartheta_6) - \ell_1 \cos(\vartheta_4), \\ J_3^5 = \ell_2 \cos(\vartheta_4) \sin(\vartheta_5) \cos(\vartheta_6) + a_3 \cos(\vartheta_4) \sin(\vartheta_5), \\ J_3^6 = -\ell_2 \sin(\vartheta_4) \cos(\vartheta_6) + \ell_2 \cos(\vartheta_4) \cos(\vartheta_5) \sin(\vartheta_6). \end{cases} \quad (5)$$

We refer to [15, 18–21] for more details on the analysis of mechanical design of this model.

The manipulability index of the current robotic manipulator was found to range between 0.7 and 1 using the Monte Carlo approach [14, 20]. This indicates that there is an inverse kinematic solution and that the manipulator is operable throughout the full work area.

We denote the link velocities as $V = [v_x^p \ v_y^p \ v_z^p \ \omega_x^p \ \omega_y^p \ \omega_z^p]^T$. This depicts the relationship between the robot's first and last links' velocities. In Figure 1, the reference states are depicted.

From equation (5), we can write

$$d\bar{A} = \begin{bmatrix} 1 & 0 & 0 & 0 & \ell_5 \cos(\vartheta_5) & \ell_5 \sin(\vartheta_5) \\ 0 & \cos(\vartheta_5 \vartheta_6) & \sin(\vartheta_5 \vartheta_6) & -\ell_5 \cos(\vartheta_6) & 0 & 0 \\ 0 & -\sin(\vartheta_5 \vartheta_6) & \cos(\vartheta_5 \vartheta_6) & \ell_5 \sin(\vartheta_6) & 0 & 0 \\ 0 & 0 & 0 & 1 & 0 & 0 \\ 0 & 0 & 0 & 0 & \cos(\vartheta_{56}) & \sin(\vartheta_{56}) \\ 0 & 0 & 0 & 0 & -\sin(\vartheta_{56}) & \cos(\vartheta_{56}) \end{bmatrix}, \quad (6)$$

where $\vartheta_{56} = \vartheta_5 + \vartheta_6$.

By using the Jacobean body geometry, we may determine this:

$$V_{p_{ba}} = [d\tilde{A}.T_5, d\tilde{A}.T_6] = \begin{bmatrix} 0 & 0 \\ -\ell_5 \cos(\vartheta_6) & 0 \\ \ell_5 \sin(\vartheta_6) & 0 \\ 1 & 1 \\ 0 & 0 \\ 0 & 0 \end{bmatrix}, \quad (7)$$

where T_5 and T_6 represent the joint 5 and 6's respective constant velocity twists. One can see [19–22] for further details.

For a given position and orientation of the tool end tip, the deformation of the prismatic joints and the rotational orientations of the rotary joints of the robot manipulators must be determined using the inverse kinematic solution. The manipulator's position control and trajectory planning can both benefit from using the inverse kinematic model.

The robot velocity of end effector $\dot{V}_{p_{a0}}$ of the moving point p_a with respect to inertial point p_0 is given by

$$E\dot{V}_{p_{a0}} = d\tilde{A}.\tilde{A}.V_{p_{a0}} + V_{p_{ba}}, \quad (8)$$

where $d\tilde{A}$ is the adjoint map given by

$$d\tilde{A} = \begin{bmatrix} R_{ba} & p_{ba}R_{ba} \\ 0 & R_{ba} \end{bmatrix}, \quad (9)$$

where R_{ba} is the rotation matrix that determines how p_a is oriented in relation to p_0 and p_{ba} is the vector that connects p_a to p_b .

Choosing of variable is extremely advantageous for controlling the links' velocity since it leads to the separation of the kinematic and dynamic components.

$$\begin{bmatrix} 1 & 0 & 0 & 0 & 0 & 0 \\ 0 & 1 & 0 & 0 & 0 & 0 \\ 0 & 0 & 100 & 70 & 0 & 0 \\ 0 & 0 & 0 & 495 & 70 & 0 \\ 0 & 0 & 0 & 0 & 0 & 0 \\ 0 & 0 & 0 & 0 & 0 & 0 \end{bmatrix} \begin{bmatrix} \dot{v}_x^p \\ \dot{v}_y^p \\ \dot{v}_z^p \\ \dot{w}_x^p \\ \dot{w}_y^p \\ \dot{w}_z^p \end{bmatrix} = \begin{bmatrix} 1 & 0 & 0 & 0 & \ell_5 \cos(\vartheta_5) & \ell_5 \sin(\vartheta_5) \\ 0 & \cos(\vartheta_5\vartheta_6) & \sin(\vartheta_5\vartheta_6) & -\ell_5 \cos(\vartheta_6) & 0 & 0 \\ 0 & -\sin(\vartheta_5\vartheta_6) & \cos(\vartheta_5\vartheta_6) & \ell_5 \sin(\vartheta_6) & 0 & 0 \\ 0 & 0 & 0 & 1 & 0 & 0 \\ 0 & 0 & 0 & 0 & \cos(\vartheta_{56}) & \sin(\vartheta_{56}) \\ 0 & 0 & 0 & 0 & -\sin(\vartheta_{56}) & \cos(\vartheta_{56}) \end{bmatrix} \begin{bmatrix} v_x^p \\ v_y^p \\ v_z^p \\ w_x^p \\ w_y^p \\ w_z^p \end{bmatrix} + \begin{bmatrix} 0 & 0 \\ -\ell_5 \cos(\vartheta_6) & 0 \\ \ell_5 \sin(\vartheta_6) & 0 \\ 1 & 1 \\ 0 & 0 \\ 0 & 0 \end{bmatrix} \begin{bmatrix} u_1 \\ u_2 \end{bmatrix},$$

$$= \begin{bmatrix} 1 & 0 & 0 & 0 & (a+b) & 0 \\ 0 & \cos(\vartheta_5\vartheta_6) & \sin(\vartheta_5\vartheta_6) & -(a+b)\cos(\vartheta_{56}) - \ell_5 \cos(\vartheta_6) & 0 & 0 \\ 0 & -\sin(\vartheta_5\vartheta_6) & \cos(\vartheta_5\vartheta_6) & (a+b)\sin(\vartheta_{56}) + \ell_5 \sin(\vartheta_6) & 0 & 0 \\ 0 & 0 & 0 & 1 & 0 & 0 \\ 0 & 0 & 0 & 0 & \cos(\vartheta_{56}) & \sin(\vartheta_{56}) \\ 0 & 0 & 0 & 0 & -\sin(\vartheta_{56}) & \cos(\vartheta_{56}) \end{bmatrix} \begin{bmatrix} v_x^p \\ v_y^p \\ v_z^p \\ w_x^p \\ w_y^p \\ w_z^p \end{bmatrix} + \begin{bmatrix} 0 & 0 \\ -\ell_5 \cos(\vartheta_6) & 0 \\ \ell_5 \sin(\vartheta_6) & 0 \\ 1 & 1 \\ 0 & 0 \\ 0 & 0 \end{bmatrix} \begin{bmatrix} u_1 \\ u_2 \end{bmatrix},$$

$$y = \begin{bmatrix} 0 & 1 & 0 & 0 & 1 & 0 \\ 0 & 0 & 0 & 0 & 0 & 1 \end{bmatrix} \begin{bmatrix} v_x^p \\ v_y^p \\ v_z^p \\ w_x^p \\ w_y^p \\ w_z^p \end{bmatrix}. \quad (10)$$

Hence, DAC-SYS is given by

$$\begin{aligned} E\dot{x} &= Ax + Bu, \\ y &= Cx. \end{aligned} \quad (11)$$

Thus, the findings in this section can be used to the analysis and development of control rules for mechanically limited manipulators, such as the surgical robots of Raven and da Vinci [22, 23].

3. Reduced Representation with Insertion Consistent Initial Algebraic Constraints

Recalling from Section 2, the developed robotic system can be modeled as a time-invariant DAC-SYS.

$$E\dot{x} = Ax + Bu, \quad (12)$$

$$y = Cx, \quad (13)$$

with

$$\begin{aligned} E, A &\in \mathbb{R}^{n \times n}, \\ B &\in \mathbb{R}^{n \times m}, \\ C &\in \mathbb{R}^{r \times n}, \\ x &\in c^1(\mathbb{R}^n), \\ u &= \begin{bmatrix} u_1 \\ u_2 \end{bmatrix} \in c(\mathbb{R}^m). \end{aligned} \quad (14)$$

Rank $(E) = n_0 < n$ that ensures the existence of nonsingular matrices G and H , where

$$HEG = \begin{bmatrix} I_{n_0} & 0 \\ 0 & 0 \end{bmatrix}, \quad (15)$$

which transform (12) and (13) into its dynamic decomposition equivalent form with

$$G^{-1}x = \begin{bmatrix} x_1 \\ x_2 \end{bmatrix}, x_1 \in \mathbb{R}^{n_0}, x_2 \in \mathbb{R}^{n-n_0}. \quad (16)$$

Consider

$$\begin{aligned} HAG &= \begin{bmatrix} W_1^1 & W_1^2 \\ W_2^1 & W_2^2 \end{bmatrix}, \\ HB &= \begin{bmatrix} B_1 \\ B_2 \end{bmatrix}, \\ HC &= [C_1 \quad C_2]. \end{aligned} \quad (17)$$

The dynamic composite system can now be written as

$$\dot{x}_1 = W_1^1 x_1 + W_1^2 x_2 + B_1 u, \quad (18)$$

$$0 = W_2^1 x_1, \quad (19)$$

$$y = C_1 x_1 + C_2 x_2. \quad (20)$$

Equations (18)–(20) form the Hessenberg DAC-SYS of size two with $W_2^1 W_1^2 = 0$ and $W_2^1 B_1 = 0$, and this S-LR reduction counterpart is guaranteed to have the same finite poles, input and output transformation zeros, and dynamic order as the character equation.

4. Reduction Robot System

The *Hessenberg* DAC-SYS is a particularly significant category of general differential-algebraic equations having a distinctive structure. With the manipulability control of index-two *Hessenberg* DAC-SYS, a variational formulation approach was devised.

We are now looking for a suitable function, such that the core features lead to a solution of DAC-SYS (18)–(20).

Assume that the invertible $W_2^1 W_1^1 W_1^2$ represent the Jacobean condition. As a result, by repeatedly differentiating the algebraic equation, the implicit function theorem [24, 25] can be used to estimate the unknown state x_2 until it can be estimated explicitly as

$$\begin{aligned} x_2 &= [W_2^1 W_1^1 W_1^2]^{-1} [-W_2^1 W_1^1 W_1^1 x_1 - W_2^1 W_1^1 B_1 u] \\ &= -v^{-1} W_2^1 W_1^1 W_1^1 x_1 - v^{-1} W_2^1 W_1^1 B_1 u, \end{aligned} \quad (21)$$

where $v = W_2^1 W_1^1 W_1^2$; then, the reduced robot system can be a dynamic equation defined on consistent initial algebraic constraints.

$$\dot{x}_1 = (1 - W_2^1 v^{-1} W_2^1 W_1^1) W_1^1 x_1 + (1 - v^{-1} W_2^1 W_1^1) B_1 u, \quad (22)$$

$$0 = W_2^1 x_1, \quad (23)$$

$$0 = W_2^1 W_1^1 x_1, \quad (24)$$

$$y = (C_1 - C_2 v^{-1} W_2^1 W_1^1 W_1^1) x_1 - C_2 v^{-1} W_2^1 W_1^1 B_1 u. \quad (25)$$

It is clear that the null space of W_2^1 and $W_2^1 W_1^1$ is non-empty; then, the class of consistent initial condition is dropped to become

$$\omega = \{x_1(t_0) \in \mathbb{R}^{n_0} \mid x_1(t_0) \in \text{Null}(W_2^1) \cap \text{Null}(W_2^1 W_1^1)\}. \quad (26)$$

4.1. Optimal Control Implementation. Consider that the class of admissible pairs (x_1, u) is

$$\Omega = \{(x_1, u) \in c^1(\mathbb{R}^n) \times c(\mathbb{R}^m) \text{ and } (x_1, u) \text{ satisfies (21)-(25)}\}. \quad (27)$$

Now, define

$$\begin{aligned} \mathbb{F}_{1\Omega} &= \frac{1}{2 \int_{t_0}^{t_f} \left\langle \begin{bmatrix} y \\ u \end{bmatrix}, \begin{bmatrix} K_1 & 0 \\ 0 & K_2 \end{bmatrix} \begin{bmatrix} y \\ u \end{bmatrix} \right\rangle dt} \\ &= \frac{1}{2} \int_{t_0}^{t_f} \left\langle \begin{bmatrix} (C_1 - C_2 v^{-1} W_2^1 W_1^1 W_1^1) x_1 - C_2 v^{-1} W_2^1 W_1^1 B_1 u \\ u \end{bmatrix}, \right. \\ &\quad \left. \begin{bmatrix} K_1 & 0 \\ 0 & K_2 \end{bmatrix} \begin{bmatrix} (C_1 - C_2 v^{-1} W_2^1 W_1^1 W_1^1) x_1 - C_2 v^{-1} W_2^1 W_1^1 B_1 u \\ u \end{bmatrix} \right\rangle dt, \end{aligned} \tag{28}$$

with $\{(x_1, u)\}$ convex set and $K_1, K_2 > 0$ (symmetric), and finally, we look for min $(\mathbb{F}_{1\Omega})$ on the class of admissible pairs Ω .

4.2. Variational Formulation of DAC-SYS. In this section, we will briefly examine how the reduction robot system (22)–(26) transforms into an identical variable (functional) whose crucial points are the answer to (22)–(26).

(i) Define the linear operator

$$\mathcal{L} = \begin{bmatrix} \mathcal{L}_1 \\ \mathcal{L}_2 \\ \mathcal{L}_3 \end{bmatrix}, \tag{29}$$

with

$$\mathcal{L}_1(x_1) = f_1(t), \tag{30}$$

where $\mathcal{L}_1 = ((1 - W_1^2 v^{-1} W_2^1 W_1^1) W_1^1) x_1, f_1 = (1 - v^{-1} W_2^1 W_1^1) B_1 u,$

$$\begin{aligned} \mathcal{L}_2(x_1) &= W_2^1 x_1, \\ \mathcal{L}_3(x_1) &= W_2^1 W_1^1 x_1, \end{aligned} \tag{31}$$

where the separable space $\text{Dom}(\mathcal{L}) = \{(x_1, u) \in c^1(\mathbb{R}^n) \times c(\mathbb{R}^n)\}$ has such a supremum norm that fills all the normed space in the stated domain

(ii) Definition of variational formulation in this case is challenging because of $\langle x_1, x_2 \rangle = \int_{t_0}^{t_f} x_1 x_2 dt,$ and with regard to $\langle x_1, x_2 \rangle$ and $d/dt,$ the operator \mathcal{L} is not symmetric.

Then, redefine $(x_1, x_2) = (x_1, \mathcal{L}x_2)$ to guarantee the variational formulation existence

$$\mathbb{F}_{2\Omega} = \frac{1}{2 \int_{t_0}^{t_f} \langle \mathcal{L}(x_1), \mathcal{L}(x_1) \rangle - 2 \left\langle \mathcal{L}(x_1), \begin{bmatrix} f_1 \\ 0 \\ 0 \end{bmatrix} \right\rangle dt} \tag{32}$$

The critical points of $\mathbb{F}_{2\Omega}$ are the solution of (19)–(23) over Ω only in the event that $\langle \cdot, \cdot \rangle$ does not degenerate on either the domain or the range of $\mathcal{L}(x_1, u)$

(iii) The critical points of $\mathbb{F}_{2\Omega}$ can be concluded from

$$\delta \mathbb{F}_{2\Omega} = \mathbb{F}_{2\Omega}(x_1 + \delta x_1, u + \delta u) - \mathbb{F}_{2\Omega}(x_1, u) |_{\text{linear part of the variation}} = 0. \tag{33}$$

(iv) $\mathbb{F}_{1\Omega}$ and $\mathbb{F}_{2\Omega}$ are quadratic in x_1 and u

(v) Since (x_1, u) is certain and positive in relation to $\langle \cdot, \cdot \rangle,$ then minimum of $\mathbb{F}_{2\Omega}$ is the solution of (22)–(26)

(vi) Since the Banach space is separable in the solvable topological space $C(\mathbb{R}^n),$ suppose that ϕ_i, ψ_i are linearly independent basis functions. Afterwards, the variable x_1, u can be defined as a finite linear combination of these basis functions:

$$\begin{aligned} x_1 &= \sum_{i=1}^{m1} \alpha_i^j \phi_i^j; j = 1, \dots, n_0, m1 > 0, \\ u &= \sum_{i=0}^{m2} \beta_i^k \psi_i^k; k = 1, \dots, m, m2 > 0. \end{aligned} \tag{34}$$

Derive $\mathbb{F}(\alpha_i^j, \beta_i^k)$ in relation to its unidentified parameters α_i^j, β_i^k and set the outcome to zero:

$$\implies \frac{\partial \mathbb{F}}{\partial \alpha_i^j} = 0, \frac{\partial \mathbb{F}}{\partial \beta_i^k} = 0, \forall i, j, k. \tag{35}$$

An approximation of a solution to DAC-SYS is then formed by solving the acquired system of linear algebraic equations.

5. Numerical Illustration

Using the findings of the inverse kinematic analysis in equations (12) and (13) and also some design parameters, including the link lengths and lower limb anatomic parameters, the objective of our study would be to design an S-LR manipulator which satisfied the specifications for comprehensive fracture fragment alignment with in target operation. The design parameters can be defined as follows:

$$\begin{aligned}
E &= \begin{bmatrix} 1 & 0 & 0 & 0 & 0 & 0 \\ 0 & 1 & 0 & 0 & 0 & 0 \\ 0 & 0 & 100 & 70 & 0 & 0 \\ 0 & 0 & 0 & 495 & 70 & 0 \\ 0 & 0 & 0 & 0 & 0 & 0 \\ 0 & 0 & 0 & 0 & 0 & 0 \end{bmatrix}, \\
A &= \begin{bmatrix} 1 & 0 & 0 & 0 & 223 & 171 \\ 0 & 1.553 & 67.45 & 3.842 & 0 & 0 \\ 0 & -67.45 & 1.553 & 233 & 0 & 0 \\ 0 & 0 & 0 & 1 & 0 & 0 \\ 0 & 0 & 0 & 0 & 1.553 & 67.45 \\ 0 & 0 & 0 & 0 & -67.45 & 1.553 \end{bmatrix}, \\
B &= \begin{bmatrix} 0 & 0 \\ 4.542 & 0 \\ 66.23 & 0 \\ 1 & 1 \\ 0 & 0 \\ 0 & 0 \end{bmatrix}, \\
C &= \begin{bmatrix} 0 & 1 & 0 & 0 & 1 & 0 \\ 0 & 0 & 0 & 0 & 0 & 1 \end{bmatrix}.
\end{aligned} \tag{36}$$

Rank $(E) = 4 < n$; this lead us to use singular value decomposition to compute U which is orthonormal eigenvectors of EE^T , and V is orthonormal eigenvectors of E^TE .

Set $G = V$ and $H = U^{-1}$.

Under the transformation (G, H) , DAC-SYS (12) and (13) can be expressed as follows:

$$\begin{aligned}
\dot{x}_1 &= W_1^1 x_1 + W_1^2 x_2 + B_1 u, \\
0 &= W_2^1 x_1, \\
y &= C_1 x_1 + C_2 x_2,
\end{aligned} \tag{37}$$

with

$$\begin{aligned}
W_1^1 &= \begin{bmatrix} -0.604 & 0.012 & 60.00 & -9.883 \\ -0.031 & 0.002 & 98.94 & 17.01 \\ 0.030 & -0.042 & 0 & 0 \\ 0.0076 & 0.038 & 0 & 0 \end{bmatrix}, \\
W_1^2 &= \begin{bmatrix} -0.211 & -0.034 \\ -0.221 & 0.001 \\ 0 & 0 \\ 0 & 0 \end{bmatrix},
\end{aligned}$$

$$\begin{aligned}
W_2^2 &= \begin{bmatrix} 0 & 0 \\ 0 & 0 \end{bmatrix}, \\
W_2^1 &= \begin{bmatrix} 0 & 0 & 1 & 0 \\ 0 & 0 & 0 & 1 \end{bmatrix}, \\
C_1 &= \begin{bmatrix} 0 & 0 & 1 & 0 \\ 0 & 0 & 0 & 0 \end{bmatrix}, \\
C_2 &= \begin{bmatrix} 1 & 0 \\ 0 & 1 \end{bmatrix}, \\
x_1 &= \begin{bmatrix} x_{11} \\ x_{12} \\ x_{13} \\ x_{14} \end{bmatrix}, \\
x_2 &= \begin{bmatrix} x_{21} \\ x_{22} \end{bmatrix}, \\
u &= \begin{bmatrix} u_1 \\ u_2 \end{bmatrix}.
\end{aligned} \tag{38}$$

According to $W_2^1 W_1^2 = 0$, $W_2^2 B_1 = 0$, the performance index is obtained:

$$\mathbb{F} = W_2^1 x_1(t_0) + W_2^2 W_1^1 x_1(t_0) + \int_{t_0}^{t_f} (\eta_1 \mathbb{F}_{1\Omega} + \eta_2 \mathbb{F}_{2\Omega}) dt. \tag{39}$$

$\mathbb{F}_{1\Omega}$ and $\mathbb{F}_{2\Omega}$ are given in Section 3.

$$\eta_1 = \eta_2 = \frac{1}{4}. \tag{40}$$

All the states are measurable.

Set

$$\begin{aligned}
x_1 &= \sum_{i=1}^5 \alpha_i^j t_i, j = 1, \dots, n_0, \\
u_1 &= \sum_{i=0}^5 \beta_i^k t_i, k = 1, \dots, n_0, \\
u_2 &= \sum_{i=0}^5 \gamma_i^k t_i, k = 1, \dots, m - n_0.
\end{aligned} \tag{41}$$

Derive $\mathbb{F}(\alpha_i^j, \beta_i^k)$ with respect to its unknown parameters α_i^j, β_i^k and equalize the result to zero.

Overall, the system behaved smoothly, allowing the user to fully manage the endoscope through the selection of parameters. The system also stayed steady during all selections (see Figure 2). In comparison to the intended trajectory, the system's inaccuracy was rather tiny (see Figure 3).

Using the aforementioned parameters, a MATLAB simulation was employed to invade the manipulator workspace. The simulation results are shown in Figures 2 and 3.

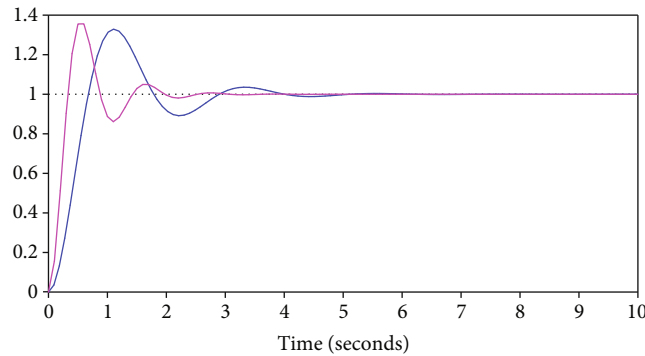
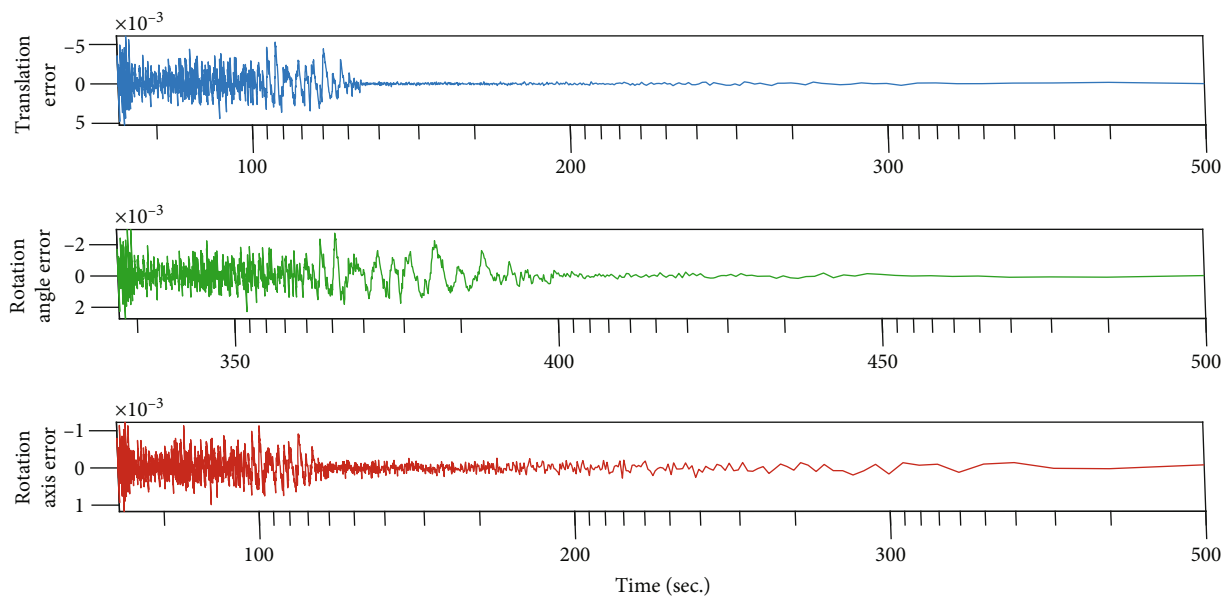
FIGURE 2: Optimal control u .

FIGURE 3: System performance errors under numerical control.

6. Conclusions

This contribution provides the necessary tools for addressing linear mechanical differential-algebraic systems. The focus was primarily on analysing the forward and inverse kinematics of the developed robotic manipulator to support femoral shaft fracture reduction surgery, thereby enhancing the safety of the S-LR system. The manipulator's design incorporates three rotational joints and three prismatic joints.

The results of the workspace study and kinematic analyses demonstrate that the mechanism can access any location within the specified workspace using the given design parameters. Modelling the mechanical system naturally leads to differential-algebraic systems, which can be explored using variational methods. It is assumed that the solvability space is a separate Banach space to ensure the existence of a countable linearly independent set of functions. The method is based on utilising the implicit function theorem and differentiation index. The differentiation index is repeatedly used to solve the algebraic equations for the unknown

state-space parameters and generate reduced-order dynamic equations defined on a class of coherent initial algebraic constraints. The average operating time was approximately 7 minutes, while the time required for the S-LR system to stabilise was around 6 seconds, demonstrating the efficiency of the proposed method.

In this particular case, the system is expressed using an operator from the variant formulation, and the solution is presented as a linear combination of basis components from the setting space. The simulation of the S-LR reduction system is performed using MATLAB software to ensure the validity and accuracy of this technique.

7. Future works

Planned future work includes the following:

- (i) There is a plan to investigate the dynamics of the joints in the robotic system to further enhance the safety of S-LR

- (ii) In the case of nonlinear mechanical systems, the theory of nonlinear DAC-SYS is yet to be developed

Data Availability

All the data is within the text.

Conflicts of Interest

The author declares that there are no conflicts of interest regarding the publication of this paper.

Acknowledgments

The author would like to thank Mustansiriyah University (<http://www.uomustansiriyah.edu.iq>), Baghdad, Iraq, for its moral support in the present work.

References

- [1] H. S. Shaymaa, A. S. Nadia, and A. Z. Radhi, "A reliable numerical algorithm for stabilizing of the 2-dimensional logistic hypercaotic trajectory," *Al-Mustansiriyah Journal of Science*, vol. 33, no. 1, pp. 51–56, 2022.
- [2] C. W. Gear and L. R. Petzold, "ODE methods for the solution of differential/algebraic systems," *SIAM Journal on Numerical Analysis*, vol. 21, no. 4, pp. 716–728, 1984.
- [3] F. A. Ghazwa and A. Z. Radhi, "Approximate solution of a reduced-type index-k Hessenberg differential-algebraic control system," *Journal of Applied Mathematics*, vol. 2021, Article ID 9706255, 13 pages, 2021.
- [4] G. Michael and Y. Wagner, "Index concepts for linear mixed systems of differential-algebraic and hyperbolic-type equations," *SIAM Journal on Scientific Computing*, vol. 22, no. 5, pp. 1610–1622, 2001.
- [5] H. A. Almurib, H. F. Al-Qrimli, and N. Kumar, "A review of application industrial robotic design," in *2011 Ninth International Conference on ICT and Knowledge Engineering*, vol. 11, pp. 105–112, Bangkok, Thailand, 2012.
- [6] Y. Tan, Z. Fu, L. Duan, R. Cui, and R. Wu, "Hill-based musculoskeletal model for a fracture reduction robot," *The International Journal of Medical Robotics and Computer Assisted Surgery*, vol. 17, no. 3, pp. 1–14, 2021.
- [7] B. Fuchtmeier, S. Egersdoerfer, R. Mai et al., "Reduction of femoral shaft fractures in vitro by a new developed reduction robot system 'RepoRobo'," *Injury*, vol. 35, no. 1, pp. 113–119, 2004.
- [8] M. N. Alam, O. A. Ilhan, J. Manafian, M. I. Asjad, H. Rezazadeh, and H. M. Baskonus, "New results of some of the conformable models arising in dynamical systems," *Advances in Mathematical Physics*, vol. 2022, Article ID 7753879, 13 pages, 2022.
- [9] F. Soltanian, M. Dehghan, and S. M. Karbassi, "Solution of differential algebraic equations via homotopy perturbation method and their engineering applications," *International Journal of Computer Mathematics*, vol. 87, no. 9, pp. 1950–1974, 2019.
- [10] J. D. Akinfenwa, S. A. Okunuga, and R. I. Abdulganiy, "Hihger oder extended block hybrid second derivatives backward differentiation formula for solving Dae of index 1,2, and 3 R. A. Soneye, O. A. Akinfenwa, R. I. Abdulganiy and S. A. Okunuga," *Research Square*, vol. 1, no. 1, pp. 1–21, 2022.
- [11] F. A. Ghazwa, "Functional approach for solving reduced order of index-four Hessenberg differential-algebraic control system," *Journal of Mathematics*, vol. 2022, Article ID 9621026, 12 pages, 2022.
- [12] N. H. Nabaa and J. A. Zainab, "Analytic approach for solving system of fractional differential differential equation," *Al-Mustansiriyah Journal of Science*, vol. 32, no. 4, pp. 14–17, 2021.
- [13] M. Golchian, M. Gachpazan, and S. H. Tabasi, "A new approach for computing the exact solutions of DAEs in generalized Hessenberg forms," *International Journal of Nonlinear Analysis and Applications*, vol. 11, no. 1, pp. 199–206, 2020.
- [14] H. B. Choi and J. Ryu, "Singularity analysis of a four degree-of-freedom parallel manipulator based on an expanded 6×6 Jacobian matrix," *Mechanism and Machine Theory*, vol. 57, no. 3, pp. 51–61, 2021.
- [15] N. Vahrenkamp and T. Asfour, "Representing the robot's workspace through constrained manipulability analysis," *Autonomous Robots*, vol. 38, no. 1, pp. 17–30, 2015.
- [16] B. I. Akinnukawe, O. A. Akinfenwa, and S. A. Okunuga, "Hybrid block algorithm for solving differential-algebraic equations with hessenberg index 3," *FUTA Journal of Research in Sciences*, vol. 15, no. 1, pp. 32–39, 2019.
- [17] B. Benhammouda, "The differential transform method as an effective tool to solve implicit Hessenberg index-3 differential-algebraic equations," *Journal of Mathematics*, vol. 2023, Article ID 3620870, 13 pages, 2023.
- [18] T. Essomba and S. N. Phu, "Kinematic analysis and design of a six-degrees of freedom 3-RRPS mechanism for bone reduction surgery," *Journal of Medical Devices*, vol. 15, no. 1, pp. 1–15, 1953.
- [19] O. O. Adewale, D. Shen, X. Wang, L. Li, and T. Zhao, "Experimental measurement of force, torque control and vibration absorber system for intraoperative tele-operated robotic-assisted femoral shaft drilling using air-controlled soft balloon damper," *Transactions of the Institute of Measurement and Control*, vol. 43, no. 11, pp. 2525–2539, 2021.
- [20] W. F. Xu, J. T. Zhang, B. Liang, and B. Li, "Singularity analysis and avoidance for robot manipulators with nonspherical wrists," *IEEE Transactions on Industrial Electronics*, vol. 63, no. 1, pp. 277–290, 2016.
- [21] A. Hijazi, J. F. Brethe, and D. Lefebvre, "Singularity analysis of a planar robotic manipulator: application to an XY-theta platform," *Mechanism and Machine Theory*, vol. 100, no. 1, pp. 104–119, 2016.
- [22] L. Sun and C. Yeung, "Port placement and pose selection of the da Vinci surgical system for collision-free intervention based on performance optimization," in *2007 IEEE/RSJ International Conference on Intelligent Robots and Systems*, vol. 1, pp. 1951–1956, San Diego, CA, USA, 2007.
- [23] B. Hannaford, J. Rosen, D. W. Friedman et al., "Raven-II: an open platform for surgical robotics research," *IEEE Transactions on Biomedical Engineering*, vol. 60, no. 4, pp. 954–959, 2013.
- [24] F. Magri, "Vatitional formulation for every linear equation," *International Journal of Engineering Science*, vol. 12, no. 6, pp. 537–549, 1974.
- [25] S. Seishi and M. Nobuyuki, "Implicit function theorem and Jacobians in solvation and adsorption," *Physica A: Statistical Mechanics and its Applications*, vol. 570, no. 1, pp. 1–30, 2021.